

SMU-HEP-13-21

A N_F -Dependent VFNS for Heavy Flavors: Merging the FFNS and VFNS

A. Kusina^{*a}, F. I. Olness^a, I. Schienbein^b, T. Jezo^d, K. Kovařík^c, T. Stavreva^b, J. Y. Yu^b

^a*Southern Methodist University, Dallas, TX 75275, USA*

^b*Laboratoire de Physique Subatomique et de Cosmologie, Université Joseph Fourier/CNRS-IN2P3/INPG, 53 Avenue des Martyrs, 38026 Grenoble, France*

^c*Institute for Theoretical Physics, Karlsruhe Institute of Technology, Karlsruhe, D-76128, Germany*

^d*Department of Physics, University of Durham, Durham DH1 3LE, UK*

Department of Mathematical Sciences, University of Liverpool, Liverpool L69 3BX, UK

E-mail: akusina@smu.edu, olness@smu.edu, schien@lpsc.in2p3.fr, T.Jezo@liverpool.ac.uk, kovarik@particle.uni-karlsruhe.de, stavreva@lpsc.in2p3.fr, yu@physics.smu.edu

We introduce a Hybrid Variable Flavor Number Scheme (H-VFNS) for heavy flavors, which incorporates the advantages of both the traditional Variable Flavor Number Scheme (VFNS) as well as the Fixed Flavor Number Scheme (FFNS). We include an explicit dependence on number of active flavors N_F in both the Parton Distribution Functions (PDFs) and the strong coupling constant α_s . This results in sets of coexisting PDFs and α_s for $N_F = \{3, 4, 5, 6\}$, that are related analytically by the $\overline{\text{MS}}$ matching conditions. The H-VFNS resums the heavy quark contributions and provides the freedom to choose the optimal N_F for each particular data set. Thus, we can fit selected HERA data in a FFNS framework, while retaining the benefits of the VFNS to analyze LHC data at high scales. We illustrate how such a fit can be implemented for the case of both HERA and LHC data.

*XXI International Workshop on Deep-Inelastic Scattering and Related Subjects
22-26 April, 2013
Marseilles, France*

^{*}Speaker.

1. Introduction

For precision analyses of collider data, the heavy quarks (charm, bottom, and top) must be properly taken into account; this is a non-trivial task due to the different mass scales which enter the theory. There are two general frameworks used for this purpose: (i) Fixed Flavor Number Scheme (FFNS), and (ii) Variable Flavor Number Scheme (VFNS).¹

In the FFNS, heavy quarks are treated as extrinsic to the proton and there are no heavy quark PDFs; they are produced only in the final state or in loops.² The advantage of the FFNS is the exact treatment of final state kinematics, which is crucial near the heavy quark production threshold. However, it is not Infra-Red (IR) safe and cannot be extended to asymptotic scales ($\mu \gg m_Q$) because of the large unresummed logarithms $\log(\mu/m_Q)$.

The VFNS is a set of multiple FFNS schemes with different numbers of active flavors N_F , that are connected by matching conditions. The matching of the N_F and N_{F+1} schemes is performed at a matching scale $\mu_M^{(N_F)}$, and this is traditionally set to the heavy quark mass m_Q . Thus, for μ scales above the heavy quark mass, a corresponding heavy quark PDF appears and resums $\log(\mu/m_Q)$ terms; this ensures the IR safety of the scheme. There are multiple implementations of the VFNS including: ACOT [5–9], TR [10, 11], FONLL [12, 13], GJR/JR [14, 15]; for recent reviews see, e.g. refs. [16–18].

In this contribution we present a new heavy flavor scheme, denoted as the Hybrid Variable Flavor Number Scheme (H-VFNS), which incorporates the advantages of both the traditional VFNS as well as the FFNS. The H-VFNS was introduced in ref. [19] and for more details we refer reader to this reference.

2. Hybrid Variable Flavor Number Scheme

We generalize the traditional VFNS by introducing an explicit dependence on the number of active flavors, N_F , in both the PDFs $f_a(x, \mu, N_F)$ and the strong coupling $\alpha_s(\mu, N_F)$:

$$\begin{aligned} f_i(x, \mu) &\longrightarrow f_i(x, \mu, N_F) \\ \alpha_s(\mu) &\longrightarrow \alpha_s(\mu, N_F). \end{aligned}$$

Thus, in the H-VFNS we have the freedom to choose the N_F value at each μ scale; this is in contrast to the traditional VFNS where the N_F value is uniquely determined by the μ scale. The H-VFNS is illustrated schematically in Fig. 1 where we explicitly see the coexistence of PDFs and α_s for different $N_F = \{3, 4, 5, 6\}$ values.

On a technical level, in addition to the *matching scale* $\mu_M^{(N_F)}$, we introduce a separate switching scale $\mu_S^{(N_F)}$. The matching scale is a μ point where we define the $N_F + 1$ PDFs and α_s in terms of the N_F ones (using the $\overline{\text{MS}}$ matching conditions). The **switching scale** $\mu_S^{(N_F)}$ is the μ scale where we change between N_F and $N_F + 1$ scheme when calculating physical observables (e.g., $d\sigma$, F_2).

¹We refer here to the General Mass (GM) VFNS, where the mass effects are included; this is in contrast to the Zero Mass (ZM) VFNS, where heavy quarks are treated as massless.

²See refs. [1, 2] for a discussion on the details of the different formulations of the FFNS. Additionally an example of PDF global analysis in the FFNS can be found for instance in refs. [3, 4].

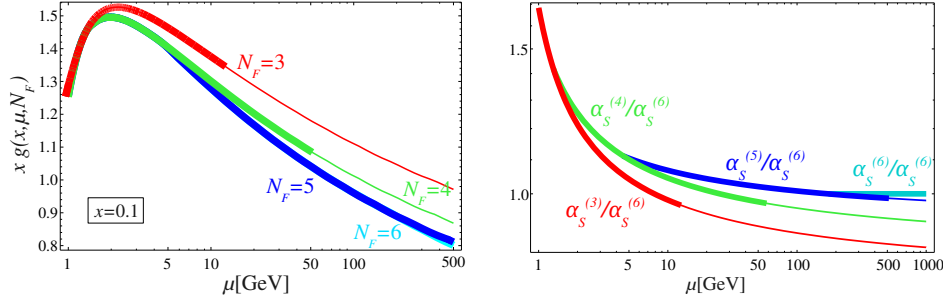


Figure 1: Schematic of a H-VFNS: PDF (left) and α_s (right) vs. μ . The preferred range of each N_F branch is indicated by the thicker line.

Below the switching scale ($\mu < \mu_S^{(N_F)}$) *physical observables* are calculated in the N_F -flavor scheme, and above the switching scale ($\mu_S^{(N_F)} < \mu$) they are calculated in the $(N_F + 1)$ -flavor scheme. In contrast, in the traditional VFNS the matching and the switching scales are equal. Indeed, in all practical applications to date these scales have been identified with the heavy quark masses: $\mu_M^{(N_F)} = \mu_S^{(N_F)} = m_{N_F}$.

The H-VFNS PDFs and α_s for different number of flavors are connected analytically by the $\overline{\text{MS}}$ matching conditions [20]. Therefore, by knowing the PDFs for a specific N_F branch, we are able to compute the related PDFs for any other number of active flavors.

Similar goal has been achieved in the frameworks of MSTW [1, 21], ABKM/ABM [3] and NNPDF [22, 23] by providing sets with different numbers of active flavors that are also connected by the $\overline{\text{MS}}$ matching conditions. Their phenomenological implications have been recently investigated in refs. [24, 25].

2.1 Problems resolved

Since PDFs and strong couplings with different N_F coexist, it allows us to avoid dealing with a N_F flavor transition should it happen to lie right in the middle of a data set. For example, if we analyze the HERA F_2^{charm} data (e.g. [26]) which covers a typical range of $Q \sim [3, 8]$ GeV and we were to use the traditional VFNS, then the N_F transition between 4 and 5 flavors would lie right in the middle of the analysis region; clearly this is very inconvenient for the analysis. Because we can specify the number of active flavors N_F in the H-VFNS, we have the option to *not* activate the b -quark in the analysis even when $\mu > m_b$; instead, we perform all our calculations of F_2^{charm} using $N_F = 4$ flavors. This will avoid any potential discontinuities in the PDFs and α_s in contrast to the traditional VFNS which forces a transition to $N_F = 5$ at the b -quark mass. Also since 4 and 5-flavor PDFs are connected analytically, it allows us to use the $N_F = 4$ PDFs extracted from the F_2^{charm} data set and relate this to $N_F = 5$ PDFs that can be applied at high μ scales for LHC processes. Note that in this example all the HERA F_2^{charm} data (both above and below m_b) influence the $N_F = 5$ PDFs used for the LHC processes.

Additionally, the H-VFNS implementation gives the user maximum flexibility in choosing where to switch between the N_F and $N_F + 1$ calculations. Not only can one choose different switching points for different processes (as sketched above), but we can make the switching point dependent on the kinematic variables of the process. For example, the production thresholds

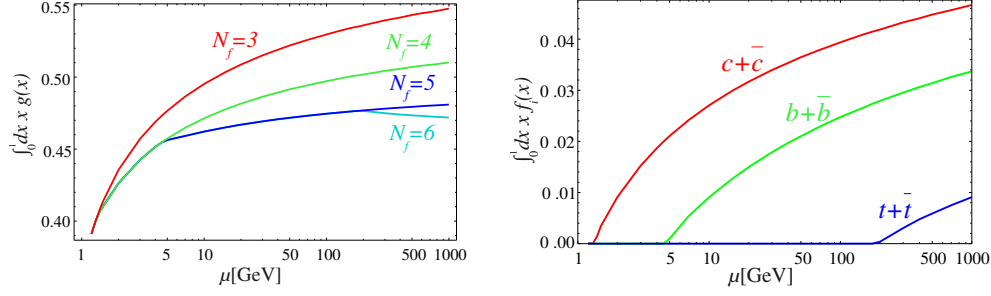


Figure 2: (a) Gluon momentum fraction; (b) Momentum fraction for $c + \bar{c}$, $b + \bar{b}$ and $t + \bar{t}$ quarks.

for charm/bottom quarks in DIS are given in terms of the photon-proton center of mass energy $W^2 \simeq Q^2(1-x)/x$; thus, we could use this to define our switching scales.

An important operational question is: how far above the $\mu = m_Q$ can we reliably extend a particular N_F framework. We know this will have mass singular logs of the form $\alpha_s \ln(\mu/m_Q)$, so these will eventually spoil the perturbation expansion. We just need to ensure that we transition to the $N_F + 1$ result before these logs obviate the perturbation theory. In general, we find that when the μ scale is more than a few times the heavy quark mass then we need to be concerned with the resummation of these logarithms [19].

3. N_F Dependence of the PDFs

One of the simplest quantities to illustrate the effect of the number of active flavors N_F on the PDFs $f_i(x, \mu, N_F)$, is the momentum fraction $\left[\int_0^1 x f_i(x) dx \right]$ carried by the PDF flavors.

Figure 2 shows the gluon and heavy quark momentum fractions as a function of the μ scale. For very low μ scales all the curves coincide by construction; when $\mu < m_{c,b,t}$ the charm, bottom, and top degrees of freedom will “deactivate” and the $N_F = 4, 5, 6$ results will reduce to the $N_F = 3$ result. As we increase the μ scale, we open up new channels. For example, when $\mu > m_c$ the charm channel activates and the DGLAP evolution will generate a charm PDF via the $g \rightarrow c\bar{c}$ process. Because the overall momentum sum rule must be satisfied $\left[\sum_i \int_0^1 x f_i(x) dx = 1 \right]$, as we increase the momentum carried by the charm quarks, we must decrease the momentum carried by the other partons. This interplay is evident in Fig. 2. In Figure 2(a), we see that for $\mu = 1000$ GeV, the momentum fraction of the $N_F = 4$ gluon is decreased by $\sim 4\%$ as compared to the $N_F = 3$ gluon. Correspondingly, in Fig. 2(b) we see that at $\mu = 1000$ GeV, the momentum fraction of the charm PDF is $\sim 4\%$. Thus, when we activate the charm in the DGLAP evolution, this depletes the gluon and populates the charm PDF via $g \rightarrow c\bar{c}$ process. The same holds for 5 and 4-flavor gluon and bottom quark.

The gluon PDF is primarily affected by the heavy N_F channels as it couples via the $g \rightarrow c\bar{c}, b\bar{b}, t\bar{t}$ processes. The effect on the light quarks $\{u, d, s\}$ is minimal as these only couple to the heavy quarks via higher order processes ($u\bar{u} \rightarrow g \rightarrow c\bar{c}$).

4. An Example: From Low to High Scales

We now finish with an example of how the H-VFNS scheme could be employed for a simultaneous study of both a low-scale process ($\mu \sim m_b$) at HERA and a high scale process ($\mu \gg m_{c,b}$) at the LHC.

At HERA, a characteristic Q range for the extraction of F_2^{charm} , for example, is $\sim [2, 10]$ GeV and this spans the kinematic region where the charm and bottom quarks become active in the PDF. These analyses can be performed using a $N_F = 3$ FFNS calculation as the scales involved are not particularly large compared to the $m_{c,b}$ scales. Actually, the extraction of the F_2^{charm} structure function is often computed using the HVQDIS program [27], and this uses a $N_F = 3$ FFNS. Conversely, at the LHC, the μ range for the new particle searches in the Drell-Yan process can be in excess of a TeV. For this analysis, we would want to use $N_F = 5$ so that the charm and bottom logs are resummed. Because the H-VFNS simultaneously provides $N_F = \{3, 4, 5, 6\}$, we can analyze the HERA data in a FFNS $N_F = 3$ context while also analyzing the LHC data in a $N_F = \{4, 5, 6\}$ VFNS context. Operationally, we could perform a PDF fit to both a combination of HERA and LHC data by implementing the following steps.

1. Parametrize the PDFs at a low initial scale $\mu = Q_0 \sim 1$ GeV, and generate a family of N_F dependent PDFs.
2. Fit the HERA F_2^{charm} structure function data using $N_F = 3$ “FFNS” PDFs, $f_i(x, \mu, N_F = 3)$ and $\alpha_s(\mu, N_F = 3)$.
3. Fit the high-scale LHC data using $N_F = 4, 5, 6$ “VFNS” PDFs, $f_i(x, \mu, N_F = 4, 5, 6)$ and $\alpha_s(\mu, N_F = 4, 5, 6)$.
4. Repeat steps 1) through 3) until we have a suitable minimum.

Note, because we generate all the PDFs and α_s for all $N_F = \{3, 4, 5, 6\}$ flavors in step 1), the separate N_F branches are analytically related. Also because we have access to all $N_F = \{3, 4, 5, 6\}$ sets, there is no difficulty in performing the HERA analysis of step 2) and the LHC analysis of step 3) in different N_F frameworks.

Finally, the user is now responsible for ensuring each N_F calculation is *not* used beyond its range of validity. While it is now possible to compute with $N_F = 3$ at high μ scales, this is not necessarily a reliable result.

4.1 N_F Conversion Factors

Finally, we demonstrate how to use the family of N_F dependent PDFs to estimate the effect of changing from $N_F = 3$ to $N_F = 5$ in a calculation such as the extraction of F_2^{charm} discussed above. For example, the HVQDIS program [27] uses a $N_F = 3$ FFNS while many of the PDFs are only available for $N_F = 4, 5$. If we have access to both $N_F = 3$ and $N_F = 5$ PDFs, we can simply use the correct N_F PDF set, and the conversion between the different N_F sets is simply given by the following identity: $f^{(N_F=5)}(x) = f^{(N_F=3)}(x)[f^{(N_F=5)}(x)/f^{(N_F=3)}(x)]$. The term in brackets above represents the “correction factor” in converting between $N_F = 3$ and $N_F = 5$ PDF sets. As we noted in Sec. 3, the dominant effect of changing from $N_F = 3$ to $N_F = 5$ was to deplete the gluon

PDF which fed the charm PDF via the $g \rightarrow c\bar{c}$ process. Therefore, we can estimate this effect by comparing the shift of the gluon PDF for $N_F = 3$ and $N_F = 5$. So even if we do not have access to both the $N_F = 3$ and $N_F = 5$ PDF sets, the combination $[f^{(N_F=5)}/f^{(N_F=3)}]$ is driven by the DGLAP evolution and only mildly sensitive to the detailed PDF; hence, the above technique can still provide a rough approximation as to the correction factor between the $N_F = 3$ and $N_F = 5$ PDFs.

5. Conclusion

We have investigated the N_F dependence of the PDFs and proposed an extension of the traditional VFNS which we denote the H-VFNS. In this scheme, we include an explicit N_F dependence in both the PDFs $f_a(x, \mu, N_F)$ and strong coupling $\alpha_s(\mu, N_F)$; this provides the user the freedom, and responsibility, to choose the appropriate N_F values for each data set and kinematic region. Thus, the H-VFNS provides a valuable tool for fitting data across a wide variety of processes and energy scales from low to high.

Acknowledgments

We thank Sergey Alekhin, Michiel Botje, John Collins, Kateria Lipka, Pavel Nadolsky, Voica Radescu, Randall Scalise, and the members of the HERA-Fitter group for valuable discussions. F.I.O., I.S., and J.Y.Y. acknowledge the hospitality of CERN, DESY, Fermilab, and Les Houches where a portion of this work was performed. This work was partially supported by the U.S. Department of Energy under grant DE-FG02-13ER41996, and the Lighter Sams Foundation. The research of T.S. is supported by a fellowship from the Théorie LHC France initiative funded by the CNRS/IN2P3. This work has been supported by *Projet international de coopération scientifique* PICS05854 between France and the USA. T.J. was supported by the Research Executive Agency (REA) of the European Union under the Grant Agreement number PITN-GA-2010-264564 (LHCPhenoNet).

References

- [1] A. Martin, W. Stirling, and R. Thorne, *Phys.Lett.* **B636** (2006) 259–264, [hep-ph/0603143](#).
- [2] M. Gluck and E. Reya, *Mod.Phys.Lett.* **A22** (2007) 351–354, [hep-ph/0608276](#).
- [3] S. Alekhin, J. Blumlein, S. Klein, and S. Moch, *Phys.Rev.* **D81** (2010) 014032, [0908.2766](#).
- [4] M. Gluck, P. Jimenez-Delgado, and E. Reya, *Eur.Phys.J.* **C53** (2008) 355–366, [0709.0614](#).
- [5] M. A. G. Aivazis, F. I. Olness, and W. K. Tung, *Phys. Rev.* **D50** (1994) 3085–3101, [hep-ph/9312318](#).
- [6] M. Aivazis, J. C. Collins, F. I. Olness, and W.-K. Tung, *Phys.Rev.* **D50** (1994) 3102–3118, [hep-ph/9312319](#).
- [7] J. C. Collins, *Phys.Rev.* **D58** (1998) 094002, [hep-ph/9806259](#).
- [8] M. Kramer, F. I. Olness, and D. E. Soper, *Phys.Rev.* **D62** (2000) 096007, [hep-ph/0003035](#).
- [9] W.-K. Tung, S. Kretzer, and C. Schmidt, *J.Phys.* **G28** (2002) 983–996, [hep-ph/0110247](#).

- [10] R. Thorne and R. Roberts, *Phys.Lett.* **B421** (1998) 303–311, [hep-ph/9711223](#).
- [11] R. Thorne, *Phys.Rev.* **D73** (2006) 054019, [hep-ph/0601245](#).
- [12] M. Cacciari, M. Greco, and P. Nason, *JHEP* **9805** (1998) 007, [hep-ph/9803400](#).
- [13] S. Forte, E. Laenen, P. Nason, and J. Rojo, *Nucl.Phys.* **B834** (2010) 116–162, [1001.2312](#).
- [14] M. Gluck, P. Jimenez-Delgado, E. Reya, and C. Schuck, *Phys.Lett.* **B664** (2008) 133–138, [0801.3618](#).
- [15] P. Jimenez-Delgado and E. Reya, *Phys.Rev.* **D80** (2009) 114011, [0909.1711](#).
- [16] R. Thorne and W. Tung, [0809.0714](#).
- [17] F. Olness and I. Schienbein, *Nucl.Phys.Proc.Suppl.* **191** (2009) 44–53, [0812.3371](#).
- [18] SM and NLO Multileg Working Group Collaboration, J. Andersen *et al.*, [1003.1241](#).
- [19] A. Kusina, F. Olness, I. Schienbein, T. Jezo, K. Kovarik, T. Stavreva, and J. Y. Yu, *Phys.Rev.* **D88** (2013) 074032, [1306.6553](#).
- [20] M. Buza, Y. Matiounine, J. Smith, and W. van Neerven, *Eur.Phys.J.* **C1** (1998) 301–320, [hep-ph/9612398](#).
- [21] A. Martin, W. Stirling, R. Thorne, and G. Watt, *Eur.Phys.J.* **C70** (2010) 51–72, [1007.2624](#).
- [22] R. D. Ball, V. Bertone, F. Cerutti, L. Del Debbio, S. Forte, *et al.*, *Nucl.Phys.* **B849** (2011) 296–363, [1101.1300](#).
- [23] R. D. Ball, V. Bertone, S. Carrazza, C. S. Deans, L. Del Debbio, *et al.*, *Nucl.Phys.* **B867** (2013) 244–289, [1207.1303](#).
- [24] R. Thorne, *Phys.Rev.* **D86** (2012) 074017, [1201.6180](#).
- [25] The NNPDF Collaboration Collaboration, R. D. Ball *et al.*, *Phys.Lett.* **B723** (2013) 330–339, [1303.1189](#).
- [26] H1 Collaboration Collaboration, A. Aktas *et al.*, *Eur.Phys.J.* **C45** (2006) 23–33, [hep-ex/0507081](#).
- [27] B. Harris and J. Smith, *Phys.Rev.* **D57** (1998) 2806–2812, [hep-ph/9706334](#).